

Ring-Opening of a Furyl Group Appended to the Cyclopentadienyl Ligand in Rare-Earth Metal Half-Sandwich Complexes

Julia Hitzbleck and Jun Okuda*

Institute of Inorganic Chemistry, RWTH Aachen University, Landoltweg 1, D-52074 Aachen, Germany

Received February 23, 2007

A series of scandium, lutetium, and yttrium complexes containing a tetramethylcyclopentadienyl ligand with a pendant furyl group, $[\text{Ln}\{\eta^5\text{-C}_5\text{Me}_4\text{SiMe}_2(\text{C}_4\text{H}_2\text{RO-2})\}(\text{CH}_2\text{SiMe}_3)_2(\text{THF})]$ ($\text{Ln} = \text{Sc, Lu, Y}$; $\text{R} = \text{H, Me}$), have been synthesized and structurally characterized. Single-crystal X-ray diffraction studies of the scandium complexes $[\text{Sc}\{\eta^5\text{-C}_5\text{Me}_4\text{SiMe}_2(\text{C}_4\text{H}_2\text{RO-2})\}(\text{CH}_2\text{SiMe}_3)_2(\text{THF})]$ ($\text{R} = \text{H, Me}$) revealed a pseudo-four-coordinate metal center without additional coordination of the furyl group. The previously elusive lutetium complex $[\text{Lu}\{\eta^5\text{-C}_5\text{Me}_4\text{SiMe}_2(\text{C}_4\text{H}_2\text{MeO-2})\}(\text{CH}_2\text{SiMe}_3)_2(\text{THF})]$ could be isolated and exhibited structural features analogous to those of the scandium compound. Variable-temperature ^1H NMR spectroscopic studies of the entire series confirmed the labile nature of both the THF ligands and furyl donor in solution. Rates for the ring-opening reaction, triggered by intramolecular C–H bond activation, were shown to depend primarily on the metal size. The ring-opening reaction resulted in the formation of the corresponding dinuclear yne–enolate complexes $[\text{Ln}\{\eta^5\text{-}\eta^1\text{-C}_5\text{Me}_4\text{SiMe}_2(\text{C}\equiv\text{CCH}=\text{CRO})\}(\text{CH}_2\text{-SiMe}_3)_2]$ ($\text{Ln} = \text{Sc, Lu, Y}$; $\text{R} = \text{H, Me}$). Substitution at the 5-furyl position did not markedly influence the rate of the ring-opening reaction but shifted the position of the monomer–dimer equilibrium toward the monomer. Only a large excess of THF allowed the observation of monomeric yne–enolate complexes such as $[\text{Y}\{\eta^5\text{-}\eta^1\text{-C}_5\text{Me}_4\text{SiMe}_2(\text{C}\equiv\text{CCH}=\text{CHO})\}(\text{CH}_2\text{SiMe}_3)(\text{THF})_2]$, which was characterized by X-ray crystallography. Addition of THF increased the stability of the lutetium bis(alkyl) complexes and allowed the formation of the corresponding cationic compounds by treatment with $[\text{NEt}_3\text{H}][\text{BPh}_4]$ to yield $[\text{Lu}\{\eta^5\text{-}\eta^1\text{-C}_5\text{Me}_4\text{SiMe}_2(\text{C}_4\text{H}_2\text{RO-2})\}(\text{CH}_2\text{SiMe}_3)(\text{THF})_n][\text{BPh}_4]$ ($\text{Ln} = \text{Lu}$; $\text{R} = \text{H, Me}$), which resisted ring-opening of the furyl group.

Introduction

The rare-earth metal centers in half-sandwich complexes are electronically and sterically less saturated than those in metallocene complexes^{1,2} and show reactivity distinct from that observed for the latter.³ Intra- and intermolecular C–H bond activation via σ -bond metathesis, particularly well documented for lanthanocene alkyl complexes, has also been reported for half-sandwich complexes.^{2a,b} For the monocationic complexes,^{1j,k} the active species proposed for homogeneous olefin polymerization catalysis based on mono(cyclopentadienyl) systems, this

reactivity pattern is also pronounced. Along with the tendency to undergo ligand redistribution reactions, C–H bond activation is made responsible for the fast catalyst degradation.^{2a,4} We have selected furyl-substituted cyclopentadienyl ligands as typical hemi-labile ligand systems⁵ and investigated the stability and reactivity of these complexes. Rare-earth metal complexes have previously been reported to yield ortho-metalation products with aromatic heterocycles such as furan, thiophene, and pyridine.⁶ Unexpectedly, with the furan group appended to the cyclopentadienyl ligand the metalation does not proceed at the 2-position but rather involves the ring proton in the 3-position, resulting

* To whom correspondence should be addressed. Tel. +49 241 80 94645. Fax: +49 241 80 92644. E-mail: jun.okuda@ac.rwth-aachen.de.

(1) (a) Edelmann, F. T., In *Comprehensive Organometallic Chemistry II*; Abel, E. W., Stone, F. G. A., Wilkinson, G., Eds.; Pergamon Press: London, 1995; Vol. 4, p 11. (b) Edelmann, F. T. *Top. Curr. Chem.* **1996**, *179*, 247. (c) Kilimann, U.; Edelmann, F. T. *Coord. Chem. Rev.* **1995**, *141*, 1. (d) Richter, J.; Edelmann, F. T. *Coord. Chem. Rev.* **1996**, *147*, 373. (e) Gun'ko, Y.; Edelmann, F. T. *Coord. Chem. Rev.* **1996**, *156*, 1. (f) Edelmann, F. T.; Gun'ko, Y. K. *Coord. Chem. Rev.* **1997**, *165*, 163. (g) Edelmann, F. T.; Lorenz, V. *Coord. Chem. Rev.* **2000**, *209*, 99. (h) Schaverien, C. J. *Adv. Organomet. Chem.* **1994**, *36*, 283. (i) Schumann, H.; Meese-Marktscheffel, J. A.; Esser, L. *Chem. Rev.* **1995**, *95*, 865. (j) Zeimentz, P. M.; Arndt, S.; Elvidge, B. R.; Okuda, J. *Chem. Rev.* **2006**, *106*, 2404. (k) Arndt, S.; Okuda, J. *Adv. Synth. Catal.* **2005**, *347*, 339.

(2) For reviews, see: (a) Arndt, S.; Okuda, J. *Chem. Rev.* **2002**, *102*, 1953. (b) Okuda, J. *Dalton Trans.* **2003**, 2367. (c) Hou, Z.; Luo, Y.; Li, X. *J. Organomet. Chem.* **2006**, *691*, 3114. For recent work on half-sandwich polymerization catalysts based on group 3 metals, see: (d) Luo, Y.; Baldamus, J.; Hou, Z. *J. Am. Chem. Soc.* **2004**, *126*, 13910. (e) Li, X.; Hou, Z. *Macromolecules* **2005**, *38*, 6767. (f) Li, X.; Baldamus, J.; Hou, Z. *Angew. Chem., Int. Ed.* **2005**, *44*, 962. (g) Cui, D.; Nishiura, M.; Hou, Z. *Macromolecules* **2005**, *38*, 4089. (h) Zhang, L.; Luo, Y.; Hou, Z. *J. Am. Chem. Soc.* **2005**, *127*, 14562. (i) Henderson, L. D.; MacInnis, G. D.; Piers, W. D.; Parvez, M. *Can. J. Chem.* **2004**, *82*, 162.

(3) (a) Watson, P. L. *J. Am. Chem. Soc.* **1982**, *104*, 337. (b) Watson, P. L. *J. Am. Chem. Soc.* **1983**, *105*, 6491. (c) Watson, P. L. *Chem. Commun.* **1983**, 276. (d) Watson, P. L.; Parshall, G. W. *Acc. Chem. Res.* **1985**, *18*, 51. (e) Thompson, M. E.; Baxter, S. M.; Bulls, A. R.; Burger, B. J.; Nolan, M. C.; Santarsiero, B. D.; Schaefer, W. P.; Bercaw, J. E. *J. Am. Chem. Soc.* **1987**, *109*, 203. (f) Hajela, S.; Bercaw, J. E. *Organometallics* **1994**, *13*, 1147. (g) Evans, W. J.; Davies, B. L. *Chem. Rev.* **2002**, *102*, 2119. (h) Evans, W. J.; Champagne, T. M.; Ziller, J. W. *J. Am. Chem. Soc.* **2006**, *128*, 14270. (i) Evans, W. J.; Davies, B. L.; Champagne, T. M.; Ziller, J. W. *Proc. Natl. Acad. Sci.* **2006**, *103*, 12678.

(4) Booi, M.; Meetsma, A.; Teuben, J. H. *Organometallics* **1991**, *10*, 3246.

(5) (a) Okuda, J. *Comments Inorg. Chem.* **1994**, *16*, 185. (b) Siemeling, U. *Chem. Rev.* **2000**, *100*, 1495.

(6) (a) den Haan, K. H.; Wielstra, Y.; Teuben, J. H. *Organometallics* **1987**, *6*, 2053. (b) Evans, W. J.; Ulibarri, T. A.; Ziller, J. W. *Organometallics* **1991**, *10*, 134. (c) Deelman, B.-J.; Booi, M.; Meetsma, A.; Teuben, J. H.; Kooijman, H.; Spek, A. L. *Organometallics* **1995**, *14*, 2306. (d) Radu, N. S.; Buchwald, S. L.; Scott, B.; Burns, C. J. *Organometallics* **1996**, *15*, 3913. (e) Ringelberg, S. N.; Meetsma, A.; Hessen, B.; Teuben, J. H. *J. Am. Chem. Soc.* **1999**, *121*, 6082. (f) Ringelberg, S. N.; Meetsma, A.; Troyanov, S. I.; Hessen, B.; Teuben, J. H. *Organometallics* **2002**, *21*, 1759. (g) Arndt, S.; Elvidge, B. R.; Zeimentz, P. M.; Spaniol, T. P.; Okuda, J. *Organometallics* **2006**, *25*, 793.

Chart 1. Rare-Earth-Metal Half-Sandwich Bis(alkyl) Complexes Discussed in This Work

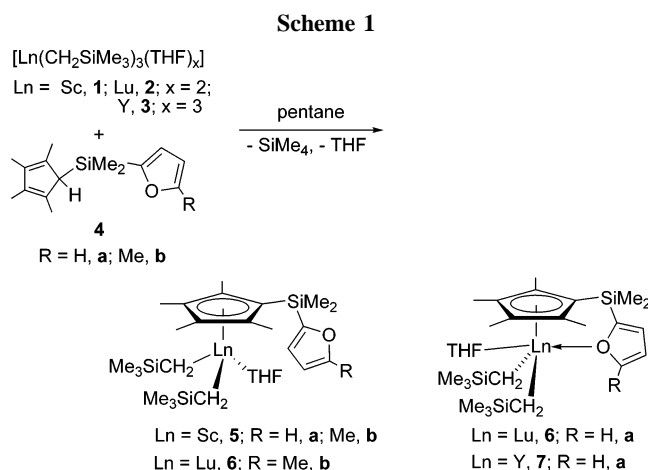
Reagents	Product
[Sc(CH ₂ SiMe ₃) ₃ (THF) ₂] (1)	
+ 4a	[Sc{η ⁵ -C ₅ Me ₄ SiMe ₂ (C ₄ H ₃ O-2)}(CH ₂ SiMe ₃) ₂ (THF)] (5a) [Sc{η ⁵ :η ¹ -C ₅ Me ₄ SiMe ₂ (C≡CCH=CHO)}(CH ₂ SiMe ₃) ₂ (THF)] (5a')
+ 4b	[Sc{η ⁵ -C ₅ Me ₄ SiMe ₂ (C ₄ H ₂ MeO-2)}(CH ₂ SiMe ₃) ₂ (THF)] (5b) [Sc{η ⁵ :η ¹ -C ₅ Me ₄ SiMe ₂ (C≡CCH=CMeO)}(CH ₂ SiMe ₃) ₂ (THF)] (5b')
[Lu(CH ₂ SiMe ₃) ₃ (THF) ₂] (2)	
+ 4a	[Lu{η ⁵ -C ₅ Me ₄ SiMe ₂ (C ₄ H ₃ O-2)}(CH ₂ SiMe ₃) ₂ (THF)] (6a) ⁷ [Lu{η ⁵ :η ¹ -C ₅ Me ₄ SiMe ₂ (C≡CCH=CHO)}(CH ₂ SiMe ₃) ₂] (6a*)
+ 4b	[Lu{η ⁵ -C ₅ Me ₄ SiMe ₂ (C ₄ H ₂ MeO-2)}(CH ₂ SiMe ₃) ₂ (THF)] (6b) ⁷ [Lu{η ⁵ :η ¹ -C ₅ Me ₄ SiMe ₂ (C≡CCH=CMeO)}(CH ₂ SiMe ₃) ₂ (THF)] (6b') [Lu{η ⁵ :η ¹ -C ₅ Me ₄ SiMe ₂ (C≡CCH=CMeO)}(CH ₂ SiMe ₃) ₂] (6b*) ⁷
[Y(CH ₂ SiMe ₃) ₃ (THF) ₃] (3)	
+ 4a	[Y{η ⁵ -C ₅ Me ₄ SiMe ₂ (C ₄ H ₃ O-2)}(CH ₂ SiMe ₃) ₃ (THF)] (7a) ⁷ [Y{η ⁵ :η ¹ -C ₅ Me ₄ SiMe ₂ (C≡CCH=CHO)}(CH ₂ SiMe ₃) ₃ (THF)] (7a*) [Y{η ⁵ :η ¹ -C ₅ Me ₄ SiMe ₂ (C≡CCH=CHO)}(CH ₂ SiMe ₃) ₂] (7a*)
+ 4b	[Y{η ⁵ :η ¹ -C ₅ Me ₄ SiMe ₂ (C≡CCH=CMeO)}(CH ₂ SiMe ₃) ₂] (7b*) ⁷

in a ring-opening reaction of the furyl group to give yne-enolate complexes.⁷ We present here the results of a study aimed at rationalizing this unusual reactivity as a function of metal size, ionic charge, and substitution pattern in the furyl group.

Results and Discussion

Synthesis and Characterization. A series of rare-earth-metal half-sandwich complexes of the type [Ln{η⁵-C₅Me₄SiMe₂(C₄H₂RO-2)}(CH₂SiMe₃)₂(THF)] (5a–7a, 5b–7b; Ln = Sc (5) Lu (6), Y (7); R = H (a) Me (b)) (Chart 1) have been prepared in good yield in pentane by reacting the respective rare-earth metal tris(trimethylsilyl)methyl complexes [Ln(CH₂SiMe₃)₃(THF)_x]⁸ (Ln = Sc (1) Lu (2), x = 2; Ln = Y (3), x = 3) with the substituted cyclopentadienes C₅Me₄H{SiMe₂(C₄H₂RO-2)} (R = H (4a), Me (4b))⁷ at room temperature over a period of 2–6 h (Scheme 1, Chart 1). The previously elusive lutetium compound 6b⁷ could now be isolated in crystalline form under these reaction conditions, albeit in low yield. The yttrium congener 7b in this series decomposed immediately in an intramolecular C–H bond activation, triggering the formation of the thermally more stable dimeric yne-enolate product 7b* (vide infra).⁷

The solid-state structures of the scandium complexes 5a,b (Figures 1 and 2) display the typical piano-stool geometry of half-sandwich complexes. In contrast to the lutetium compound 6a reported earlier,⁷ the pendant furyl moiety does not coordinate to the scandium center. This is the result of the significantly smaller size of scandium compared with the sizes of lutetium and yttrium and, thus, the preference for a pseudo-four-coordinate metal center in 5a,b over the pseudo-five-coordinate trigonal-bipyramidal structure of 6a.⁷ Furthermore, the donor



strength of furan is lower than that of THF,^{6f,7,9} suppressing replacement of the THF donor. The argument of the unfavorable steric strain in such a chelating system does not hold in the case of the small scandium center, as the THF donor is replaced in the analogous 2-pyridyl-substituted complex [Sc{η⁵:η¹-C₅Me₄SiMe₂(C₅H₄N-2)}(CH₂SiMe₃)₂].¹⁰ This complex displays an angle between the cyclopentadienyl ring and pyridyl donor similar to that in the furyl system. Overall, the structure of 5a,b is comparable to that of related structurally characterized scandium half-sandwich complexes, e.g., [Sc(η⁵-C₅Me₄SiMe₃)(CH₂SiMe₃)₂(THF)]¹¹ and [Sc{η⁵-C₅Me₄SiMe₂(C₆F₅)}(CH₂SiMe₃)₂(THF)]¹² with the η⁵-coordinated cyclopentadienyl ring in the apical position (Sc–Cp(cent) = 2.172 Å (5a), 2.198 Å (5b)) and the remaining ligands and donors in the basal plane (Sc–C = 2.220(2)–2.2437(13) Å; Sc–O = 2.171(2) Å).

Variable-temperature ¹H NMR spectroscopic data of 5a,b did not indicate any interaction of the furyl ring with the scandium

(7) Arndt, S.; Spaniol, T. P.; Okuda, J. *Organometallics* **2003**, *22*, 775.

(8) (a) Lappert, M. F.; Pearce, R. *Chem. Commun.* **1973**, 126. (b) Hultsch, K. C.; Spaniol, T. P.; Okuda, J. *Angew. Chem., Int. Ed.* **1999**, *38*, 227. (c) Schumann, H.; Freckmann, D. M. M.; Dechert, S. *Z. Anorg. Allg. Chem.* **2002**, *628*, 2422.

(9) (a) Berthelot, M.; Besseau, F.; Laurence, C. *Eur. J. Org. Chem.* **1998**, 925. (b) Evans, W. J.; Fujimoto, C. H.; Johnston, M. A.; Ziller, J. W. *Organometallics* **2002**, *21*, 1825.

(10) Hitzbleck, J.; Okuda, J. Unpublished results.

(11) Luo, Y.; Baldamus, J.; Hou, Z. *J. Am. Chem. Soc.* **2004**, *126*, 13910.

(12) Hitzbleck, J.; Okuda, J., *Z. Anorg. Allg. Chem.* **2006**, *632*, 1947.

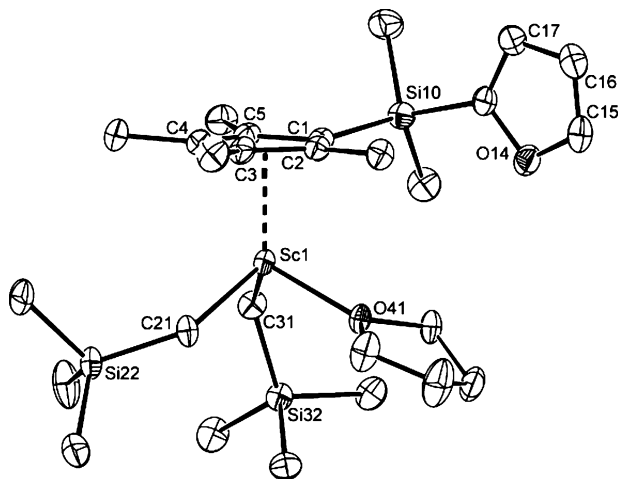


Figure 1. Molecular structure of **5a**. Hydrogen atoms have been omitted for clarity. Selected bond lengths (Å) and angles (deg): Sc–O41, 2.171(2); Sc–C21, 2.220(2); Sc–C31, 2.211(2); Sc–C(1–5), 2.478(3)–2.493(3); C21–Sc–C31, 103.92(11); C21–Sc–O41, 92.24(10); C31–Sc–O41, 105.05(9).

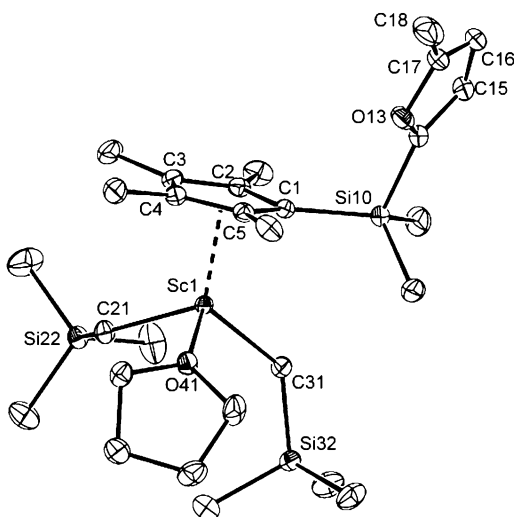


Figure 2. Molecular structure of **5b**. Hydrogen atoms have been omitted for clarity. Selected bond lengths (Å) and angles (deg): Sc–O41, 2.1709(9); Sc–C21, 2.2437(13); Sc–C31, 2.2282(13); Sc–C(1–5), 2.4799(12)–2.5411(13); C21–Sc–C31, 103.93(5); C21–Sc–O41, 95.74(4); C31–Sc–O41, 103.76(4).

metal center in solution, consistent with their solid-state structure discussed above. No characteristic shift changes of the aromatic furyl CH signals could be observed in the temperature range of -60 to $+60$ °C (Table 1), as would be expected for coordination of the furyl moiety to the Lewis acidic metal center. The methylene protons of the two CH_2SiMe_3 groups appeared as broad signals even at -60 °C, indicating a highly fluxional structure. The corresponding data for the larger congeners **6a,b** and **7a** indicated a fluxional structure in solution at room temperature with dissociatively labile THF.⁷ At -80 °C the methylene proton signals of **6a** and **7a** became diastereotopic, corresponding to a C_s -symmetric structure, and the furyl proton signals were significantly shifted downfield (Table 1). In contrast, the slightly larger steric demand of the 5-methylfuryl substituent apparently prevents such an additional stabilization in **6b**, as indicated by temperature-independent shift values for the furyl substituent. Similar to the structures of **5a,b**, no diastereotopic methylene protons were observed for **6b** at low temperature. Despite the more rigid structures of **6a** and **7a** at

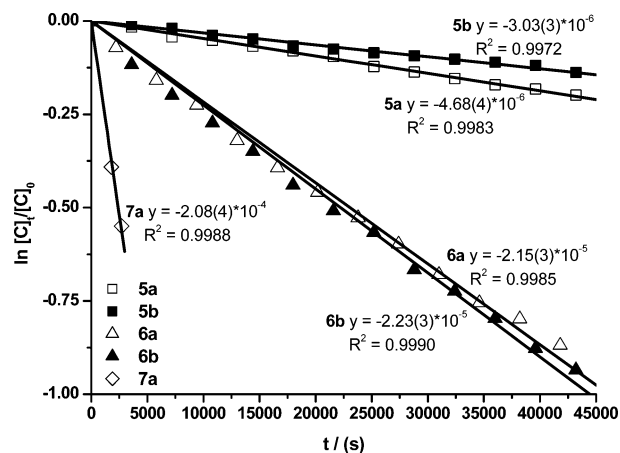


Figure 3. Logarithmic plot of furyl ring-opening via C–H bond activation in complexes **5a,b**, **6a,b**, and **7a** under yne–enolate formation.

low temperature, these complexes were still too fluxional on the NMR time scale to indicate possible agostic C–H contacts which promote the ring-opening reaction observed in solution (vide infra).

Ring-Opening of the Furyl Group. The metalation of (hetero)aromatic systems by organometallic complexes, usually in the position ortho to the heteroatom, is a well-documented reaction in the literature.^{3e,f,4,6d,f,g} The subsequent ring-opening reaction in the case of furan, on the other hand, has been reported but only studied in detail in a few cases.^{6f,7} With the aforementioned series of complexes in hand, we have now correlated the reactivity and structural trends influencing the intramolecular C–H bond activation reaction. The furyl-substituted half-sandwich complexes **5–7** showed decreasing thermal stability with increasing metal size,¹³ facilitating the ring-opening reaction of the furyl moiety in a noncoordinating solvent with yne–enolate formation (Scheme 2).

The small size of the scandium center allowed formation of the thermally stable bis(alkyl) complexes **5a,b** which only slowly converted into the corresponding yne–enolate complexes **5a'** ($t_{1/2}(40$ °C) = 41.1 h for **5a**) and **5b'** ($t_{1/2}(40$ °C) = 61.7 h for **5b**) at 40 °C (Figure 3). The slightly higher stability of **5b** can be rationalized by the higher rotation barrier of the 5-methyl-substituted furyl donor. An increase in size of the metal center by 0.116 Å¹² from scandium to lutetium led to a more pronounced tendency toward C–H bond activation in the furyl group of the corresponding complexes **6a** ($t_{1/2}(40$ °C) = 8.9 h) and **6b** ($t_{1/2}(40$ °C) = 8.6 h), but significant influence of the 5-methyl substitution at the furyl moiety could not be observed. The yttrium complexes **7a** ($t_{1/2}(40$ °C) = 0.9 h) and **7b** ($t_{1/2}(10$ °C) = 2.0 h)⁷ are even less stable, and the 5-methyl substitution of the furyl donor drastically reduced the stability in this case. Monitoring the reaction of **7a** was hampered by the decomposition of the yne–enolate complex **7a'** formed at 40 °C in solution.

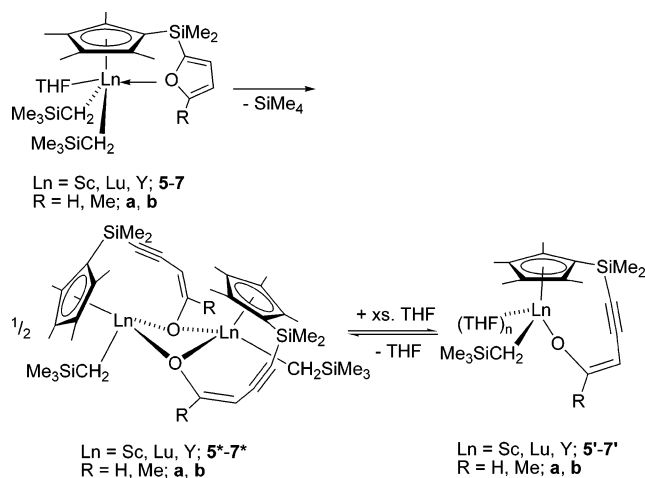
Mechanism of the Ring-Opening. The mechanism of these types of ring-opening reactions has been discussed previously for **7b**.⁷ For the formation of the related ytrocene complex $[\text{Y}(\eta^5\text{-C}_5\text{Me}_5)_2(\eta^2\text{-C}_4\text{H}_3\text{O})]$, no clear pathway for the formation of the yne–enolate complexes was proposed by Teuben et al., due to inconclusive data from kinetic experiments.^{6f} The chelate

(13) $r(\text{Sc}^{3+}) = 0.745$ Å, $r(\text{Lu}^{3+}) = 0.861$ Å, and $r(\text{Y}^{3+}) = 0.900$ Å for coordination number 6: Shannon, R. D. *Acta Crystallogr.* **1976**, A32, 751.

(14) Bambirra, S.; Meetsma, A.; Hessen, B. *Organometallics* **2006**, 25, 3486.

Table 1. Furyl Proton Signals (δ (ppm)) in the ^1H NMR Spectra of **5a,b**, **6a,b**, and **7a** in $[\text{D}_8]\text{Toluene}$ at Different Temperatures

	5a			6a			7a ⁷			5b		6b	
	H-3	H-4	H-5	H-3	H-4	H-5	H-3	H-4	H-5	H-3	H-4	H-3	H-4
+60 °C	6.49	6.14	7.53							6.50	5.83		
+25 °C	6.53	6.14	7.42	6.52	6.15	7.53	6.47	6.17	7.92	6.56	5.85	6.53	5.83
-60 °C	6.55	6.09	7.25	6.27	6.01	8.07	6.24	6.24	8.19	6.56	5.85	6.55	5.80

Scheme 2

effect of the heteroatom fragment has been proposed to be a critical factor influencing the ring-opening mechanism.⁷ Monitoring the intramolecular C–H bond activation and subsequent yne–enolate formation by ^1H NMR spectroscopy showed first-order kinetics as well as an increase in the rate of the reaction with increasing metal size (Figure 3). While this is in agreement with the higher tendency of the furyl substituent to chelate to the coordinatively unsaturated metal center of the larger metals, the 5-methyl substituent is expected to display a stronger influence on the hindered rotation. Intramolecular C–H bond activation has also been reported by Evans et al. for the related half-sandwich complex $[\text{Y}\{\eta^5\text{-C}_5\text{Me}_4\text{SiMe}_2(\text{CH}_2\text{CH}=\text{CH}_2)\}(\text{CH}_2\text{-SiMe}_3)_2(\text{THF})]$, without any significant yttrium–olefin interaction in solution.¹⁵ Nonetheless, this compound was observed to convert into $[\text{Y}\{\eta^5\text{-C}_5\text{Me}_4\text{SiMe}_2(\text{C}_3\text{H}_3)\}(\text{L})_2]$ ($\text{L} = \text{THF}, \text{DME}$) at room temperature over several days under double C–H bond activation of the allyl function by the (trimethylsilyl)methyl group with SiMe_4 elimination.¹⁵

Bercaw et al. discussed two possible transition states for the σ -bond metathesis reaction of C–H bonds of hydrocarbon fragments with aromatic C–H bonds.^{3c} C–H bond activation in a position α to an oxygen or nitrogen donor atom in the aromatic heterocycles occurs via a four-center, six-electron arrangement. Thus, a similar transition state can also be assumed when the orientation of the C–H bond is enforced by steric effects, as found for the chelating $\text{C}_5\text{Me}_4\text{SiMe}_2\text{R}$ ligands derived from **4a,b** (Scheme 3). Rotation of the pendant donor around the SiMe_2 –(2-furyl) bond orients the hydrogen in the 3-position to close proximity of the metal center.

Estimation of the Ln–H3(furyl) distance by simple rotation of the furyl group around the C_5Me_4 – SiMe_2 bond as well as the SiMe_2 –furyl bond (Scheme 3) generates close contacts which decrease with increasing metal size ($\text{Sc-H} = 2.774 \text{ \AA}$ in **5a**; $\text{Sc-H} = 2.551 \text{ \AA}$ in **5b**; $\text{Lu-H} = 2.004 \text{ \AA}$ in **6a**). This suggests that the size of the metal center and the resulting close contacts of the Ln–C and C–H bonds mainly affect the C–H bond activation rate. The effect of the 5-methyl group at the

furyl ring is probably more steric than electronic in nature. The sterically constrained scandium complexes **5a,b** hinder the rotation of the pendant donor, with slightly higher steric interactions of the methyl-substituted furyl complex leading to increased stability of **5b**. For the larger lutetium complexes **6a,b** this effect is reversed. Although both complexes display similar ring-opening rates, **6a** displays a strong Lu–O interaction in the solid state as well as in solution, while the furyl donor in **6b** is not in the vicinity of the metal center, as indicated by ^1H NMR spectroscopic data. Determination of the activation parameters of **6a,b** from an Eyring plot (Figure 4) gave: $\Delta H^\ddagger = 62.2 \pm 2.2 \text{ kJ mol}^{-1} \text{ K}^{-1}$ and $\Delta S^\ddagger = -140.2 \pm 6.6 \text{ J mol}^{-1} \text{ K}^{-1}$ for **6a** and $\Delta H^\ddagger = 88.6 \pm 2.2 \text{ kJ mol}^{-1} \text{ K}^{-1}$ and $\Delta S^\ddagger = -52.9 \pm 6.6 \text{ J mol}^{-1} \text{ K}^{-1}$ for **6b**. These data suggest an ordered transition state for the rate-determining step of the C–H activation reaction, indicated by the large negative values for the entropy of activation. The methyl-substituted donor in **6b** raises the activation enthalpy but lowers the transition state energy, leading to a slightly higher C–H bond metalation rate. For the intramolecular C–H bond activation in the 1,4,7-triazacyclononane–amide complex $[\text{La}\{\text{Pr}_2\text{TACN}(\text{SiMe}_2)\text{N}^i\text{-Bu}\}(\text{CH}_2\text{SiMe}_3)_2]$, Hessen et al. reported the activation parameters $\Delta H^\ddagger = 54.6 \pm 0.5 \text{ kJ mol}^{-1} \text{ K}^{-1}$ and $\Delta S^\ddagger = +27 \pm 20 \text{ J mol}^{-1} \text{ K}^{-1}$ as a simple first-order kinetic process.¹⁴ While the activation energies for the TACN complexes **6a,b** appear comparable, the positive entropy of activation indicates faster C–H bond activation for the larger lanthanum complex. The reported half-life of 30 min (35 °C) is in the range of that for the yttrium complex **7a**. The strong coordination of the furyl substituent allows isolation of **7a**, whereas the steric hindrance of the 5-methyl substituent in **7b** leads to concomitant formation of the C–H bond activation product **7b***, as observed in the ^1H NMR spectrum.⁷ Hence, the formation of potentially close contacts for C–H bond activation by positioning the 3-furyl ring proton in the proximity of the metal (and CH_2SiMe_3 ligand) seems to be critical. These contacts are expected to increase with the size of the metal and the need for coordinative saturation. Finally, the possibility of ring methyl metalation to give a so-called tucked-in complex prior to C–H bond activation of the 3-furyl ring proton cannot be excluded at this stage.^{1,3,4}

Complex stabilization by weak agostic C–H contacts, which subsequently result in σ -bond metathesis reactions, is reduced in the presence of a coordinating solvent. Monitoring the stability of complexes **5b** and **6b** in $[\text{D}_8]\text{THF}$ showed no signs of decomposition for **5b** at room temperature over a period of 2 weeks and very slow ring opening for **6b** ($t_{1/2}(25 \text{ °C}) = \sim 48 \text{ h}$). The retarding influence of Lewis base donors on the decomposition of hydrocarbyl complexes has been mentioned for the related complex $[\text{Y}(\eta^5\text{-C}_5\text{Me}_5)_2(\eta^2\text{-C}_4\text{H}_3\text{O})]$ upon coordination of THF.^{6f} In return, the rigid structure observed in the solid state as well as at low temperature blocks C–H contacts at the metal center and explains the reasonable stability of these compounds as crystalline solids.

Structure of an Yne–Enolate Complex. The monomeric structure of **7a'** resembles that of so-called constrained-geometry

(15) Evans, W. J.; Brady, J. C.; Ziller, J. W. *J. Am. Chem. Soc.* **2001**, *123*, 7711.

Scheme 3

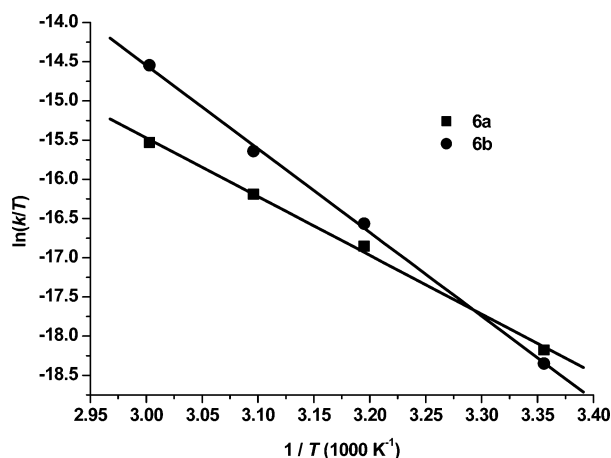
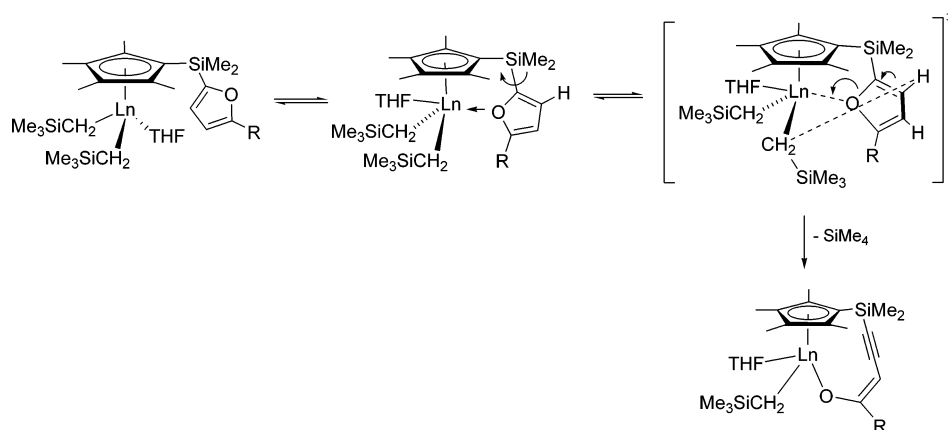


Figure 4. Eyring plot of furyl ring-opening in complexes **6a,b**.

half-sandwich complexes at first sight (Figure 5).¹⁶ However, the longer pendant yne-enolate function leads to a O–Y–C_{pcent} angle (154.87°) much wider than the close to 90° coordination of a short amido linkage, as seen, for example, in [Y{η⁵-C₅-Me₄SiMe₂(NC₅H₁₁)}](CH₂SiMe₃)(THF)].^{16a} The yne-enolate in **7a'** formally replaces one alkyl ligand in **6a**, and the additional THF donor forces the remaining alkyl group trans and the two THF donors cis to the yne-enolate. The resulting trigonal-bipyramidal structure with the cyclopentadienyl ring, enolate, and alkyl group in the equatorial plane and the two THF donors on the apices only differs from **6a** in the orientation of the ligands around the metal center. The Y–C and Y–O distances (Y–C = 2.419(3) Å, Y–C_{pcent} = 2.443 Å, Y–O(en) = 2.167(2) Å, Y–O(THF) = 2.374(2), 2.413(2) Å, CN = 7) are in the expected range,^{16a} although they are slightly longer (0.04–0.05 Å) than in the related dimeric structure of **7b***, as expected from the higher coordination number.⁷ In return, the Y–O distance is much shorter in **7a'** (0.376 Å) as a result of the enolate bridging in **7b***. The C–C distances in the yne-enolate side chain of **7a'** compare well to those in **7b*** (C–C = 1.405(7), 1.423(7) Å, C=C = 1.323(6), 1.333(6) Å, C≡C = 1.197(6), 1.226(7) Å) and the related bis(cyclopentadienyl) ynyl-enolate complex [{Y(η⁵-C₅Me₅)₂}(μ-OCH=CHC≡C)] (C–C = 1.435(14) Å, C=C = 1.323(16) Å, C≡C = 1.227(13) Å).^{6f}

Interestingly, the monomeric structure of **7a'** observed in the solid state is retained only in THF solution. ¹H NMR spectra

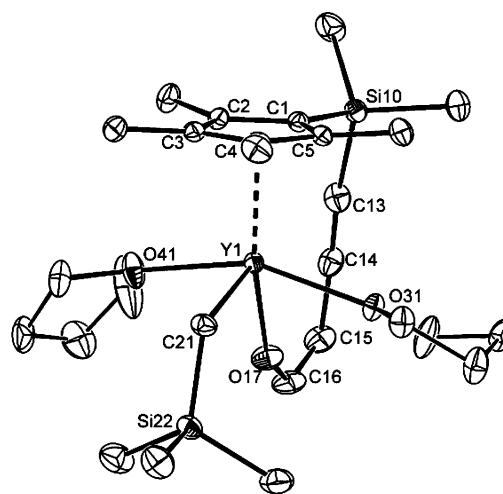


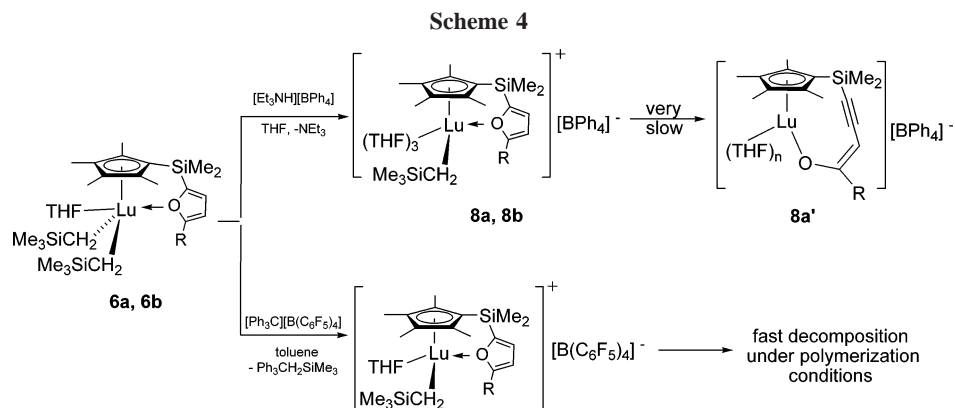
Figure 5. Molecular structure of the ring-opening product **7a'**. Hydrogen atoms have been omitted for clarity. Selected bond distances (Å) and angles (deg): Y–O17, 2.167(2); Y–O31, 2.374(2); Y–O41, 2.413(2); Y–C21, 2.419(3); Y–C(1–5), 2.662(3)–2.788(3); O31–Y–O41, 155.28(8); C21–Y–O17, 100.04(9); C21–Y–O31, 87.07(9); C21–Y–O41, 90.59(9); O17–Y–O31, 79.11(8); O17–Y–O41, 77.08(8).

in benzene indicate dimerization of **7a'** to form **7a***, similar to the behavior of the other ring-opened products **6a*** and **6b***. The dimeric structure of the unsubstituted yne-enolate in **6a*** is preferred even in the presence of excess THF (1:1 [D₆]-benzene–[D₈]THF: **6a*** (87%), **6a'** (13%)), but the slightly larger steric demand induced by the methyl substituent in **6b'** resulted in the complete formation of the monomeric species ([D₆]benzene with 1 equiv of THF per metal center: **6b'** (67%), **6b*** (33%)).

Cationic Complexes. The poor styrene polymerization activity of the precatalysts **5–7**¹⁷ could be ascribed to the tendency of the furyl group at the cyclopentadienyl ligand to undergo a ring-opening reaction in the corresponding cationic species under polymerization conditions in a weakly coordinating solvent such as toluene or bromobenzene. Due to the intermediate thermal stability of the lutetium species in this series, complexes **6a,b** were selected for the comparison of the stability of the corresponding cations. Addition of 1 equiv of the Brønsted acid [NEt₃H][BPh₄] to **6a,b** in THF resulted in clean formation of the cationic half-sandwich complexes [Lu{η⁵-C₅Me₄SiMe₂(C₄H₂-

(16) (a) Hultzsich, K. C.; Voth, P.; Beckerle, K.; Spaniol, T. P.; Okuda, J. *Organometallics* **2000**, *19*, 228. (b) Arndt, S.; Spaniol, T. P.; Okuda, J. *Eur. J. Inorg. Chem.* **2001**, 73. (c) Arndt, S.; Trifonov, A.; Spaniol, T. P.; Okuda, J.; Kitamura, M.; Takahashi, T. *J. Organomet. Chem.* **2002**, *647*, 158.

(17) Styrene polymerization experiments with **5b** and **6b** in toluene with [Ph₃C][B(C₆F₅)₄] in the presence of 10 equiv of AlⁱBu₃ produced a maximum activity of ~5 kg of sPS (mol of Ln)⁻¹ h⁻¹, with decreasing activity upon prolonged polymerization time.

**Table 2. Experimental Data for the Crystal Structure Determinations of the Complexes 5a,b and 7a'**

	5a	5b	7a'
Crystal Data			
formula	C ₂₇ H ₄₇ O ₂ ScSi ₃	C ₂₈ H ₅₃ O ₂ ScSi ₃	C ₂₇ H ₄₅ O ₃ Si ₂ Y
fw	532.88	550.93	562.72
cryst color	colorless	colorless	colorless
cryst size, mm	0.60 × 0.27 × 0.25	0.90 × 0.80 × 0.70	0.62 × 0.28 × 0.20
space group	<i>P</i> 2 ₁ / <i>c</i> (No. 14)	<i>P</i> 2 ₁ / <i>n</i> (No. 14)	<i>P</i> 2 ₁ / <i>c</i> (No. 14)
<i>a</i> , Å	18.278(10)	10.711(1)	16.875(4)
<i>b</i> , Å	9.313(5)	15.971(2)	10.176(2)
<i>c</i> , Å	19.002(10)	20.006(2)	17.594(4)
β , deg	103.093(10)	104.203(2)	99.049(6)
<i>V</i> , Å ³	3151(3)	3317.6(6)	2983.8(11)
<i>Z</i>	4	4	4
ρ_{calcd} , g cm ⁻³	1.123	1.103	1.253
μ (Mo K α), mm ⁻¹	0.368	0.351	2.059
<i>F</i> (000)	1152	1200	1192
Data Collection			
<i>T</i> , K	130(2)	143(2)	133(2)
λ , Å	0.71073	0.71073	0.71073
θ range	1.14–27.33	1.65–27.50	2.32–27.08
index ranges			
<i>h</i>	–23 to +23	–13 to +13	–15 to +21
<i>k</i>	–9 to +11	–20 to +20	–12 to +13
<i>l</i>	–21 to +24	–25 to +25	–21 to +22
Solution and Refinement			
no. of rflns measd	19 430	42 219	20 294
no. of indep rflns	6957 (<i>R</i> (int) = 0.0463)	7610 (<i>R</i> (int) = 0.0259)	6520 (<i>R</i> (int) = 0.0532)
no. of obsd rflns	5101 (<i>I</i> > 2 σ (<i>I</i>))	6894 (<i>I</i> > 2 σ (<i>I</i>))	4832 (<i>I</i> > 2 σ (<i>I</i>))
GOF	1.036	1.045	1.023
final <i>R</i> indices <i>R</i> 1, ^a w <i>R</i> 2 ^b (obsd data)	0.0532, 0.1412	0.0318, 0.0875	0.0408, 0.0934
final <i>R</i> indices <i>R</i> 1, w <i>R</i> 2 (all data)	0.0775, 0.1573	0.0358, 0.0918	0.0687, 0.1061
largest <i>e</i> (max), <i>e</i> (min), e Å ⁻³	0.739, –0.350	0.375, –0.328	0.687, –0.419

$$^a R1(F) = \sum ||F_o| - |F_c|| / \sum |F_o|. \quad ^b wR2(F) = [\sum w(F_o^2 - F_c^2)^2 / \sum w(F_o^2)]^{1/2}.$$

RO-2)}(CH₂SiMe₃)(THF)₃][BPh₄] (R = H (**8a**), Me (**8b**)) overnight (Scheme 4).

The cationic complexes **8a,b** showed high stability in THF solution (*t*_{1/2}(25 °C) = 100 days for **8a**; *t*_{1/2}(25 °C) ≫ 100 days for **8b**), even higher than that observed for the neutral complexes **6a,b** in THF. In **8a,b** three THF donors (on the basis of ¹H NMR spectroscopic data) coordinate to the metal center, one replacing the eliminated alkyl group along with one additional THF, increasing the coordination number by 1. Therefore, the metal centers in the cationic species seem to be more sterically encumbered than in the neutral dialkyl complex in THF solution. Furthermore, the lutetium complexes demonstrate the weaker Lewis base donor strength of furan in comparison with that of THF and pyridine. The ¹H NMR spectra of **8a,b** in [D₃]pyridine revealed no interaction between the furyl donor and the metal center, in agreement with a chemical shift value for the methylene protons of –0.11 ppm due to the higher donor strength of pyridine. The complexes **8a,b** in [D₈]THF showed a high-field shift of the methylene proton signal (–0.75 ppm)

and coordination of the furyl donor in **8a**, but only partial coordination (25%) of the furyl donor was observed for **8b**. Thus, the 5-methyl group seems to have a strong steric influence, restricting the rotation around the SiMe₂–furyl bond for potential coordination as well as close contacts for C–H bond activation.

Conclusion

The series of scandium, lutetium, and yttrium complexes containing a furyl-substituted cyclopentadienyl ligand showed that intramolecular C–H bond activation at the aromatic ring primarily depends on the steric and electronic saturation of the metal center. For compounds of similar overall geometry, the rate of C–H bond activation increases with increasing metal size (Y ≫ Lu > Sc). This may be a result of the increasing M–C bond polarity and thus decreasing M–C bond dissociation

enthalpy,¹⁸ concomitant with a decrease in steric saturation of the metal center. The sterically more bulky 5-methyl-substituted furyl donor hinders the free rotation of the pendant donor due to repulsion with the remaining ligands in the coordination sphere. The addition of a coordinating solvent such as THF also significantly reduces the decomposition rate, as the coordination number of the metal center increases. The fine balance between favorable steric demand and number of coordinated ligands as well as an intramolecularly coordinated donor allows the formation of stable cationic lutetium half-sandwich complexes that do not undergo significant ring opening in THF solution,⁷ whereas the parent bis(alkyl) complexes gradually decompose. In the absence of THF, as is the case during olefin polymerization, rapid decomposition of the cationic active species by C–H bond activation is likely to occur.

Experimental Section

General Remarks. All operations were carried out under argon using standard Schlenk-line and glovebox techniques. Pentane was distilled from sodium/triglyme benzophenone ketyl, THF, and toluene from sodium benzophenone ketyl under argon. NMR spectra were recorded on Varian Unity-500 (¹H, 499.6 MHz; ¹³C, 125.6 MHz), Bruker Avance II 400 MHz (¹H, 400.1 MHz; ¹³C, 100.6 MHz), and Varian Mercury-200 (¹⁹F, 188.1 MHz) spectrometers in [D₆]benzene, [D₈]THF, [D₈]toluene at 20 °C, unless stated otherwise; the chemical shifts were referenced to the residual solvent resonances. C, H analysis of crystalline samples repeatedly gave poor results with inconsistent values from run to run. This difficulty is attributed to the extreme sensitivity of the material and has been described previously.¹⁹ Metal analysis was performed by complexometric titration;²⁰ the samples (20–30 mg) were dissolved in acetone (10 mL) and titrated with EDTA (0.005 M) using xylenol orange as an indicator and ammonium acetate (1 M) as buffer solution (10 mL). The substituted cyclopentadienes **4a,b**⁷ and the complexes [Ln(CH₂SiMe₃)₃(THF)_x] (Ln = Sc (**1**), Lu (**2**), x = 2; Ln = Y (**3**), x = 3)⁸ were prepared according to literature procedures.

[Sc{η⁵-C₅Me₄SiMe₂(C₄H₃O-2)}(CH₂SiMe₃)₂(THF)] (**5a**). A solution of **4a** (0.739 g, 3.00 mmol) in pentane (10 mL) was added to **1** (1.352 g, 3.00 mmol), and the mixture was stirred at room temperature for 3 h. The solution was filtered and the solvent volume reduced to ca. 3 mL. Cooling to –40 °C gave colorless crystals of **5a** (1.417 g, 2.64 mmol); yield: 88.0%. ¹H NMR (500 MHz, [D₈]toluene): δ –0.29 (s, 4H, CH₂SiMe₃), 0.22 (s, 18H, CH₂SiMe₃), 0.59 (s, 6H, SiMe₂), 1.32 (s, 4H, β-THF), 1.94, 2.10 (s, 2 × 6H, C₅Me₄), 3.67 (s, 4H, α-THF), 6.14 (dd, ³J_{HH} = 3.4, 1.8 Hz, 1H, 4-furyl), 6.53 (d, ³J_{HH} = 3.4 Hz, 1H, 3-furyl), 7.42 (s, 1H, 5-furyl). ¹H NMR ([D₈]toluene, 60 °C): δ –0.27 (s, 4H, CH₂SiMe₃), 0.18 (s, 18H, CH₂SiMe₃), 0.55 (s, 6H, SiMe₂), 1.44 (s, 4H, β-THF), 2.00, 2.10 (s, 2 × 6H, C₅Me₄), 3.72 (s, 4H, α-THF), 6.14 (dd, ³J_{HH} = 3.4, 1.8 Hz, 1H, 4-furyl), 6.49 (d, ³J_{HH} = 3.4 Hz, 1H, 3-furyl), 7.53 (d, ³J_{HH} = 1.5 Hz, 1H, 5-furyl). ¹³C{¹H} NMR ([D₈]toluene, 60 °C): δ 0.9 (SiMe₂), 4.2 (CH₂SiMe₃), 12.1, 14.8 (C₅Me₄), 25.3 (β-THF), 41.4 (ScCH₂), 70.4 (α-THF), 110.5 (2-furyl), 112.4 (ipso-C₅Me₄), 120.9 (3-furyl), 125.4, 129.0 (C₅Me₄), 146.5 (4-furyl), 163.1 (5-furyl). ¹H NMR (–60 °C): δ –0.29 (s, 4H, CH₂SiMe₃), 0.33 (s, 18H, CH₂SiMe₃), 0.64 (s, 6H, SiMe₂), 0.98 (s, 4H, β-THF), 1.85, 2.09 (s, 2 × 6H, C₅Me₄), 3.34 (s, 4H, α-THF), 6.09 (s, 1H, 4-furyl), 6.55 (s, 1H, 3-furyl), 7.25 (s, 1H,

5-furyl). ¹³C{¹H} NMR ([D₈]toluene, –60 °C): δ 0.6 (SiMe₂), 4.6 (CH₂SiMe₃), 12.0, 14.9 (C₅Me₄), 24.9 (β-THF), 39.3 (ScCH₂), 71.2 (α-THF), 110.2 (2-furyl), 112.3 (ipso-C₅Me₄), 121.1 (3-furyl), 124.3, 128.2 (C₅Me₄), 146.43 (4-furyl), 160.1 (5-furyl). Anal. Calcd for C₂₇H₅₁O₂ScSi₃ (536.91): Sc, 8.37. Found: Sc, 8.33.

[Sc{η⁵:η¹-C₅Me₄SiMe₂(C≡CCH=CHO)}(CH₂SiMe₃)₂(THF)] (**5a**). A sample of **5a** was heated to 40 °C for 12 h. Slow conversion into the enolate complex was monitored by ¹H NMR spectroscopy. Product distribution after 12 h: **5a** (80%), **5a'** (20%). ¹H NMR of **5a'** (200 MHz, [D₈]toluene): δ –0.40 (s, 2H, CH₂SiMe₃), 0.19 (s, 9H, CH₂SiMe₃), 0.57 (s, 6H, SiMe₂), 1.40 (t, 2H, β-THF), 1.74, 1.80, 2.09, 2.21 (s, 4 × 3H, C₅Me₄), 3.50 (s, 2H, α-THF), 4.45 (d, ³J_{HH} = 5.2 Hz, 1H, 3-enolate), 6.96 (d, ³J_{HH} = 5.2 Hz, 1H, 2-enolate).

[Sc{η⁵-C₅Me₄SiMe₂(C₄H₂MeO-2)}(CH₂SiMe₃)₂(THF)] (**5b**). A solution of **4b** (0.781 g, 3.00 mmol) in pentane (10 mL) was added to **1** (1.352 g, 3.00 mmol), and the mixture was stirred at room temperature for 3 h. The solution was filtered and the solvent volume reduced to ~3 mL. Cooling to –40 °C gave colorless crystals of **5b** (1.124 g, 2.04 mmol); yield 68.0%. ¹H NMR (500 MHz, [D₆]benzene): δ –0.24 (s, 4H, CH₂SiMe₃), 0.28 (s, 18H, CH₂SiMe₃), 0.66 (s, 6H, SiMe₂), 1.22 (s, 4H, β-THF), 1.95, 2.17 (s, 2 × 6H, C₅Me₄), 2.09 (s, 3H, 5-Me-furyl), 3.64 (s, 4H, α-THF), 5.85 (s, 1H, 4-furyl), 6.56 (s, 1H, 3-furyl). ¹³C{¹H} NMR ([D₆]benzene): δ 1.0 (SiMe₂), 4.4 (CH₂SiMe₃), 12.1, 14.9 (C₅Me₄), 24.9 (β-THF), 40.6 (b, ScCH₂), 71.3 (α-THF), 106.6 (4-furyl), 113.3 (ipso-C₅Me₄), 122.2 (3-furyl), 124.8, 128.4 (C₅Me₄), 127.3 (2-furyl), 156.3 (5-furyl). ¹H NMR (500 MHz, [D₈]toluene, 60 °C): δ –0.30 (s, 4H, CH₂SiMe₃), 0.19 (s, 18H, CH₂SiMe₃), 0.61 (s, 6H, SiMe₂), 1.43 (s, 4H, β-THF), 1.98 (s, 6H, C₅Me₄), 2.15 (s, 3 + 6H, 5-Me-furyl + C₅Me₄), 3.76 (s, 4H, α-THF), 5.83 (s, 1H, 4-furyl), 6.50 (s, 1H, 3-furyl). ¹³C{¹H} NMR ([D₈]toluene, 60 °C): δ 0.8 (SiMe₂), 4.4 (CH₂SiMe₃), 12.1, 14.9 (C₅Me₄), 13.8 (Me-furyl), 25.1 (β-THF), 41.1 (ScCH₂), 71.2 (α-THF), 106.7 (2-furyl), 113.5 (ipso-C₅Me₄), 122.3 (3-furyl), 125.1, 128.6 (C₅Me₄), 156.3 (4-furyl), 159.5 (5-furyl). ¹H NMR ([D₈]toluene, –60 °C): δ –0.24 (s, 4H, CH₂SiMe₃), 0.28 (s, 18H, CH₂SiMe₃), 0.66 (s, 6H, SiMe₂), 1.22 (s, 4H, β-THF), 1.95, 2.17 (s, 2 × 6H, C₅Me₄), 2.09 (s, 3H, 5-Me-furyl), 3.64 (s, 4H, α-THF), 5.85 (s, 1H, 4-furyl), 6.56 (s, 1H, 3-furyl). ¹³C{¹H} NMR ([D₈]toluene, –60 °C): δ 0.8 (SiMe₂), 4.6 (CH₂SiMe₃), 12.0, 15.2 (C₅Me₄), 13.8 (Me-furyl), 24.9 (β-THF), 39.3 (ScCH₂), 71.2 (α-THF), 106.6 (2-furyl), 112.7 (ipso-C₅Me₄), 122.3 (3-furyl), 124.3, 128.0 (C₅Me₄), 156.2 (4-furyl), 158.3 (5-furyl). ¹H NMR (400 MHz, [D₈]THF): δ –0.43 (s, 4H, CH₂SiMe₃), 0.00 (s, 18H, CH₂SiMe₃), 0.59 (s, 6H, SiMe₂), 1.85 (s, 4H, β-THF), 2.08, 2.16 (s, 2 × 6H, C₅Me₄), 2.36 (s, 3H, 5-Me-furyl), 3.69 (s, 4H, α-THF), 6.02 (d, ³J_{HH} = 3.0 Hz, 1H, 4-furyl), 6.53 (d, ³J_{HH} = 3.0 Hz, 1H, 3-furyl). ¹³C{¹H} NMR ([D₈]THF): δ 0.2 (SiMe₂), 3.4 (CH₂SiMe₃), 11.2, 12.8 (C₅Me₄), 14.1 (Me-furyl), 24.4 (β-THF), 39.2 (b, ScCH₂), 66.1 (α-THF), 105.8 (2-furyl), 112.9 (ipso-C₅Me₄), 121.6 (3-furyl), 124.1, 127.8 (C₅Me₄), 155.9 (4-furyl), 158.2 (5-furyl). Anal. Calcd for C₂₈H₅₃O₂ScSi₃ (550.93): Sc, 8.33. Found: Sc, 8.16.

[Sc{η⁵:η¹-C₅Me₄SiMe₂(C≡CCH=CMeO)}(CH₂SiMe₃)₂(THF)] (**5b**). A sample of **5b** was heated to 40 °C for 20 h. Slow conversion into the enolate complex was monitored by ¹H NMR. Product distribution after 12 h: **5b** (84%), **5b'** (16%). ¹H NMR for **5b'** (200 MHz, [D₆]benzene): δ –0.40 (s, 2H, CH₂SiMe₃), 0.28 (s, 9H, CH₂SiMe₃), 0.53, 0.66 (s, 2 × 3H, SiMe₂), 1.30 (s, 4H, β-THF), 1.95, 2.10, 2.17, 2.30 (s, 4 × 3H, C₅Me₄), 3.64 (s, 4H, α-THF), 4.54 (s, 1H, 3-enolate).

[Lu{η⁵:η¹-C₅Me₄SiMe₂(C≡CCH=CHO)}(CH₂SiMe₃)₂(**6a***)]. A sample of **6a** was heated to 40 °C for 12 h. Slow conversion into the enolate complex was monitored by ¹H NMR. Product distribution after 12 h: **6a** (33%), **6a*** (67%). ¹H NMR for **6a*** (200 MHz, [D₈]toluene): δ –0.96, –0.51 (d, ²J_{HH} = 11.2 Hz, 2 × 2H, CH₂SiMe₃), 0.24 (s, 2 × 9H, CH₂SiMe₃), 0.46, 0.58 (s, 2 ×

(18) Schock, L. E.; Seyam, A. M.; Sabat, M.; Marks, T. J. *Polyhedron* **1988**, *7*, 1517.

(19) (a) Mitchell, J. P.; Hajela, S.; Brookhart, S. K.; Hardcastle, K. I.; Henling, L. M.; Bercaw, J. E. *J. Am. Chem. Soc.* **1996**, *118*, 1045. (b) Bambirra, S.; Brandsma, M. J. R.; Brussee, E. A. C.; Meetsma, A.; Hessen, B.; Teuben, J. H. *Organometallics* **2000**, *19*, 3197.

(20) Das, B.; Shome, S. C. *Anal. Chim. Acta* **1971**, *56*, 483.

6H, SiMe₂), 1.80, 1.86, 2.15, 2.26 (s, 4 × 6H, C₅Me₄), 4.51 (d, ³J_{HH} = 5.2 Hz, 2H, 2-enolate), 7.01 (d, ³J_{HH} = 5.3 Hz, 2H, 3-enolate). Addition of excess THF led to complete formation of [Lu{η⁵:η¹-C₅Me₄SiMe₂(C≡CCH=CHO)}(CH₂SiMe₃)₂(THF)₂] (**6a**); stepwise addition of THF led to a mixture of **6a*** and **6a'**. ¹H NMR for **6a*** (87%), **6a'** (13%), and **6a'** (200 MHz, [D₆]benzene/[D₈]-THF (1:1)): δ -1.25 (s, 2H, CH₂SiMe₃), -0.30 (s, 9H, CH₂SiMe₃), 0.40 (s, 6H, SiMe₂), 1.96, 1.98 (s, 2 × 6H, C₅Me₄), 4.28 (d, ³J_{HH} = 4.6 Hz, 1H, 2-enolate), 7.38 (d, ³J_{HH} = 4.6 Hz, 1H, 3-enolate).

[Lu{η⁵-C₅Me₄SiMe₂(C₄H₂MeO-2)}(CH₂SiMe₃)₂(THF)] (**6b**). A solution of **6b** (0.781 g, 3.00 mmol) in pentane (10 mL) was added to **2** (1.742 g, 3.00 mmol) and stirred at room temperature for 3 h. The solution was filtered and the solvent volume reduced to ~3 mL. Cooling to -40 °C gave colorless crystals of **6b** (0.480 g, 0.72 mmol); yield 24.0%. ¹H NMR (400 MHz, [D₈]-toluene): δ -0.85 (s, 4H, CH₂SiMe₃), 0.24 (s, 18H, CH₂SiMe₃), 0.61 (s, 6H, SiMe₂), 1.27 (br s, 4H, β-THF), 1.98, 2.18 (s, 2 × 6H, C₅Me₄), 2.11 (s, 3H, 5-Me-furyl), 3.60 (br s, 4H, α-THF), 5.83 (dd, ³J_{HH} = 3.1, 1.0 Hz, 1H, 4-furyl), 6.53 (d, ³J_{HH} = 3.1 Hz, 1H, 3-furyl). ¹H NMR (-80 °C): δ -0.76 (s, 4H, CH₂SiMe₃), 0.37 (s, 18H, CH₂SiMe₃), 0.67 (s, 6H, SiMe₂), 0.88 (s, 4H, β-THF), 1.89, 2.19 (s, 2 × 6H, C₅Me₄), 2.02 (s, 3H, 5-Me-furyl), 3.23 (br s, 4H, α-THF), 5.80 (dd, ³J_{HH} = 3.0, 1.0 Hz, 1H, 4-furyl), 6.56 (d, ³J_{HH} = 3.0 Hz, 1H, 3-furyl). ¹³C{¹H} NMR ([D₈]toluene, -80 °C): δ 0.9 (SiMe₂), 4.9 (CH₂SiMe₃), 11.7, 14.7 (C₅Me₄), 13.9 (Me-furyl), 24.8 (β-THF), 38.8 (s, LuCH₂), 70.6 (α-THF), 106.7 (2-furyl), 110.6 (ipso-C₅Me₄), 122.9, 126.1 (C₅Me₄), 122.2 (3-furyl), 156.3 (4-furyl), 158.6 (5-furyl). ¹H NMR (400 MHz, [D₈]THF): δ -1.12 (s, 4H, CH₂SiMe₃), -0.12 (s, 18H, CH₂SiMe₃), 0.45 (s, 6H, SiMe₂), 2.00 (s, 12H, C₅Me₄), 2.23 (s, 3H, Me-furyl), 5.90 (dd, ³J_{HH} = 3.0, 1.0 Hz, 1H, 4-furyl), 6.43 (d, ³J_{HH} = 3.0 Hz, 1H, 3-furyl). ¹³C{¹H} NMR ([D₈]THF): δ 1.0 (SiMe₂), 4.3 (CH₂SiMe₃), 12.1, 14.7 (C₅Me₄), 24.5 (β-THF), 39.3 (ScCH₂), 68.2 (α-THF), 106.5 (2-furyl), 112.6 (ipso-C₅Me₄), 117.4 (3-furyl), 123.5, 126.8 (C₅Me₄), 156.8 (4-furyl), 159.4 (5-furyl). Anal. Calcd for C₂₈H₃₅LuO₂Si₃ (680.95): Lu, 26.69. Found: Lu, 26.65.

[Lu{η⁵:η¹-C₅Me₄SiMe₂(C≡CCH=CMeO)}(CH₂SiMe₃)₂(THF)₂] (**6b'**) + [Lu{η⁵:η¹-C₅Me₄SiMe₂(C≡CCH=CMeO)}(CH₂SiMe₃)₂] (**6b***). A sample of **6b** was heated to 40 °C for 23.5 h. Slow conversion into the enolate complex was monitored by ¹H NMR. Product distribution after 12 h: **6b**, 39%; **6b'** + 0.5 **6b***, 61%. ¹H NMR (200 MHz, [D₆]benzene): **6b'**, δ -0.96 (s, 2H, CH₂-SiMe₃), 0.22 (s, 2 × 9H, CH₂SiMe₃), 0.57 (s, 6H, SiMe₂), 1.41 (s, 8H, β-THF), 1.66 (s, 3H, Me-enolate), 1.83, 2.27 (s, 2 × 6H, C₅-Me₄), 3.60 (s, 8H, α-THF), 4.48 (s, 1H, 3-enolate); **6b***, -0.76, -0.84 (d, ²J_{HH} = 11.5 Hz, 2 × 2H, CH₂SiMe₃), 0.21, 0.20 (s, 2 × 9H, CH₂SiMe₃), 0.46, 0.55 (s, 2 × 6H, SiMe₂), 1.78 (s, 6H, Me-enolate), 1.92, 1.95, 2.18, 2.23 (s, 4 × 6H, C₅Me₄), 4.48 (s, 2H, 3-enolate). Addition of excess THF led to complete formation of **6b'**.

[Y{η⁵:η¹-C₅Me₄SiMe₂(C≡CCH=CHO)}(CH₂SiMe₃)₂(THF)₂] (**7a'**). Recrystallization of **7a** (1.000 g, 1.722 mmol) from THF after stirring at 25 °C for 48 h led to the isolation of **7a'** (0.879 g, 1.562 mmol); yield: 90.7%. ¹H NMR of **7a'** (400 MHz, [D₈]-THF): δ -1.24 (d, 2H, ²J_{YH} = 3.5 Hz, CH₂SiMe₃), 0.17 (s, 9H, CH₂SiMe₃), 0.37 (d, 6H, SiMe₂), 1.96, 2.01 (s, 2 × 6H, C₅Me₄), 4.20 (d, ³J_{HH} = 4.3 Hz, 1H, OCH=CH), 7.26 (dd, ³J_{HH} = 4.3, 2.3 Hz, 1H, OCH=CH). ¹³C{¹H} NMR ([D₈]THF): δ 2.9 (SiMe₂), 4.7 (CH₂SiMe₃), 12.2, 14.6 (C₅Me₄), 26.3 (β-THF), 34.1, 34.6 (d, ¹J_{YC} = 46.0 Hz, YCH₂), 68.2 (α-THF), 80.9 (CHC≡C), 97.6 (SiC≡C), 105.7 (SiC≡C), 115.2 (ipso-C₅Me₄), 122.9, 124.3 (C₅Me₄), 170.5 (OCHCH). Dimerization to [Y{η⁵:η¹-C₅Me₄-SiMe₂(C≡CCH=CHO)}(CH₂SiMe₃)₂] (**7a***) is observed in a non-coordinating solvent. ¹H NMR for **7a*** (400 MHz, [D₆]benzene): δ -0.69, -0.23 (dd, ²J_{HH} = 11.1 Hz, ²J_{YH} = 3.7 Hz, 2H, CH₂-SiMe₃), 0.31 (s, 9H, CH₂SiMe₃), 0.44, 0.58 (d, 6H, SiMe₂), 1.41 (t, 8H, β-THF), 1.78, 1.89, 2.10, 2.33 (s, 4 × 3H, C₅Me₄), 3.58 (t,

8H, α-THF), 4.53 (d, ³J_{HH} = 5.1 Hz, 1H, OCH=CH), 6.96 (dd, ³J_{HH} = 5.1 Hz, ³J_{YH} = 2.3 Hz, 1H, OCH=CH). ¹³C{¹H} NMR ([D₆]benzene): δ 0.0, 1.2 (SiMe₂), 3.8 (CH₂SiMe₃), 10.3, 11.2, 13.2, 14.5 (C₅Me₄), 25.1 (β-THF), 34.0, 34.5 (d, YCH₂, ¹J_{YC} = 50.3 Hz), 67.1 (α-THF), 84.0 (CHC≡C), 100.4 (SiC≡C), 100.8 (SiC≡C), 115.4 (ipso-C₅Me₄), 121.4, 124.0, 125.6, 127.9 (C₅Me₄), 163.0 (OCH=CH). Anal. Calcd for C₂₇H₄₅O₃Si₂Y (562.72): Y, 15.81. Found: Y, 15.80.

[Lu{η⁵:η¹-C₅Me₄SiMe₂(C₄H₃O)}(CH₂SiMe₃)₂(THF)₃][BPh₄] (**8a**). [NEt₃H][BPh₄] (0.106 g, 0.25 mmol) and **6a** (0.167 g, 0.25 mmol) were dissolved in THF (5 mL) and stirred overnight. The product was precipitated by addition of pentane (5 mL), filtered off, and washed with pentane to give a colorless powder of **8a** (0.219 g, 0.21 mmol); yield 83.9%. ¹H NMR (400 MHz, [D₈]THF): δ -0.75 (s, 2H, CH₂SiMe₃), -0.01 (s, 9H, CH₂SiMe₃), 0.64 (s, 6H, SiMe₂), 2.10, 2.17 (s, 2 × 6H, C₅Me₄), 6.56 (dd, 1H, ³J_{HH} = 3.3, 1.8 Hz, 4-furyl), 6.81 (t, 5H, ³J_{HH} = 7.3 Hz, *p*-Ph + 3-furyl), 6.95 (t, 8H, ³J_{HH} = 7.4 Hz, *o*-Ph), 7.37 (br s, 8H, *m*-Ph), 7.76 (d, 1H, ³J_{HH} = 1.8 Hz, 2-furyl). ¹³C{¹H} NMR: δ 0.0 (CH₂SiMe₃), 3.8 (SiMe₂), 11.0, 13.6 (C₅Me₄), 25.7 (β-THF), 35.7 (LuCH₂), 67.4 (α-THF), 110.6 (ipso-C₅Me₄), 112.3 (2-furyl), 121.0 (*p*-Ph), 121.4 (3-furyl), 124.8 (*m*-Ph), 125.0, 129.2 (C₅Me₄), 146.4 (4-furyl), 136.3 (*o*-Ph), 161.3 (5-furyl), 163.6, 164.0, 164.5, 165.0 (ipso-Ph). ¹¹B NMR: δ -6.54. ¹H NMR (400 MHz, [D₅]pyridine): δ -0.11 (s, 2H, CH₂-SiMe₃), -0.01 (s, 9H, CH₂SiMe₃), 0.58 (s, 6H, SiMe₂), 1.66 (t, 12H, β-THF), 1.88, 1.93 (s, 2 × 6H, C₅Me₄), 3.70 (t, 12H, α-THF), 6.66 (dd, 1H, ³J_{HH} = 3.3 Hz, 1.5 Hz, 4-furyl), 6.93 (d, ³J_{HH} = 3.3 Hz, 3-furyl), 7.19 (t, 4H, ³J_{HH} = 7.2 Hz, *p*-Ph), 7.37 (t, 8H, ³J_{HH} = 7.4 Hz, *o*-Ph), 7.98 (d, ³J_{HH} = 1.5 Hz, 5-furyl), 8.16 (br s, 8H, *m*-Ph); ¹³C{¹H} NMR ([D₅]pyridine): δ 0.0 (CH₂SiMe₃), 3.5 (SiMe₂), 11.3, 13.7 (C₅Me₄), 25.2 (β-THF), 38.0 (LuCH₂), 67.2 (α-THF), 110.4 (ipso-C₅Me₄), 112.1 (2-furyl), 121.5 (3-furyl), 122.4 (*p*-Ph), 125.7 (*m*-Ph), 125.4, 129.3 (C₅Me₄), 136.3 (*o*-Ph), 146.7 (4-furyl), 159.7 (5-furyl), 163.8, 164.3, 164.7, 165.2 (ipso-Ph). ¹¹B NMR ([D₅]pyridine): δ -5.68. Anal. Calcd for C₅₅H₇₆BLuO₄Si₂ (1043.16): C, 63.33; H, 7.34; Lu, 16.77. Found: C, 63.86; H, 7.71; Lu, 17.21. After 2 weeks at room temperature small signals (7%) characteristic of the yne-enolate ring-opening product **8a'** appeared in [D₅]pyridine at δ 4.58 (d, 1H, ³J_{HH} = 4.5 Hz, 3-enolate) and 7.46 (d, 1H, ³J_{HH} = 4.5 Hz, 2-enolate).

[Lu{η⁵-C₅Me₄SiMe₂(C₄H₂MeO)}(CH₂SiMe₃)₂(THF)₃][BPh₄] (**8b**). [NEt₃H][BPh₄] (0.106 g, 0.25 mmol) and **6b** (0.170 g, 0.25 mmol) were dissolved in THF (5 mL) and stirred overnight. The product was precipitated by addition of pentane (5 mL), filtered off, and washed with pentane to yield a colorless powder of **8b** (0.218 g, 0.20 mmol); yield 82.5%. The NMR shows a mixture of two complexes with free and coordinating furyl donor function (chemical shift values in parentheses) in the ratio ~1:0.25. ¹H NMR ([D₈]THF): δ -0.85 (-0.87) (s, 2H, CH₂SiMe₃), -0.10 (-0.12) (s, 9H, CH₂SiMe₃), 0.47 (0.51) (s, 6H, SiMe₂), 1.97, 2.06 (s, 2 × 6H, C₅Me₄), 2.25 (s, 3H, Me-furyl), 5.96 (6.44) (dd, ³J_{HH} = 3.0, 1.0 Hz, 1H, 4-furyl), 6.46 (7.63) (dd, ³J_{HH} = 3.0, 1.0 Hz, 1H, 3-furyl), 6.80 (t, 4H, ³J_{HH} = 7.3 Hz, *p*-Ph), 6.93 (t, ³J_{HH} = 7.5 Hz, 8H, *o*-Ph), 7.35 (br s, 8H, *m*-Ph). ¹³C{¹H} NMR ([D₈]THF): δ 0.0 (CH₂SiMe₃), 3.9 (SiMe₂), 11.1, 13.5 (C₅Me₄), 12.8 (22.3) (Me-furyl), 25.4 (β-THF), 34.2 (34.9) (LuCH₂), 67.3 (α-THF), 106.2 (ipso-C₅Me₄), 113.4 (110.6) (2-furyl), 120.9 (*p*-Ph), 121.4 (3-furyl), 124.8 (*m*-Ph), 122.5, 129.2 (C₅Me₄), 125.9 (4-furyl), 136.3 (*o*-Ph), 156.2 (157.7) (5-furyl), 163.5, 164.0, 164.5, 165.0 (ipso-Ph). ¹¹B NMR ([D₈]THF): δ -6.54. ¹H NMR ([D₅]pyridine): δ -0.75 (s, 2H, CH₂SiMe₃), -0.01 (s, 9H, CH₂SiMe₃), 0.64 (s, 6H, SiMe₂), 2.07, 2.16 (s, 2 × 6H, C₅Me₄), 2.35 (s, 3H, Me-furyl), 6.27 (d, ³J_{HH} = 3.0 Hz, 1H, 4-furyl), 6.83 (d, ³J_{HH} = 3.0 Hz, 1H, 3-furyl), 6.78 (t, ³J_{HH} = 7.3 Hz, 4H, *p*-Ph), 6.93 (t, ³J_{HH} = 7.4 Hz, 8H, *o*-Ph), 7.35 (br s, 8H, *m*-Ph). ¹³C{¹H} NMR ([D₅]pyridine): δ 0.0 (CH₂SiMe₃),

3.5 (SiMe₂), 11.3, 13.8 (C₅Me₄), 13.2 (Me-furyl), 25.2 (β-THF), 38.1 (LuCH₂), 67.2 (α-THF), 106.6 (ipso-C₅Me₄), 112.9 (2-furyl), 121.8 (*p*-Ph), 122.8 (3-furyl), 125.6 (*m*-Ph), 125.3, 129.3 (C₅Me₄), 136.3 (4-furyl), 136.6 (*o*-Ph), 156.2 (5-furyl), 163.8, 164.3, 164.7, 165.3 (ipso-Ph). ¹¹B NMR ([D₅]pyridine): δ -5.67. Anal. Calcd for C₅₆H₇₈BLuO₄Si₂ (1057.18): C, 63.62; H, 7.44; Lu, 16.55. Found: C, 62.68; H, 7.22; Lu, 16.63. No signals characteristic of the yne-enolate complex were observed after 1 week.

X-ray Crystal Structure Determination. Crystallographic data for **5a,b** and **7a'** are summarized in Table 2. X-ray diffraction data were collected on a Bruker CCD area-detector diffractometer with Mo Kα radiation (graphite monochromator, λ = 0.710 73 Å) using φ and ω scans. The SMART program package was used for the data collection and unit cell determination; processing of the raw frame data was performed using SAINT; absorption corrections were applied with SADABS.²¹ The structures were solved by direct methods and refined against F² using all reflections with the

SHELXL-97 software. The non-hydrogen atoms were refined anisotropically, and hydrogen atoms were placed in calculated positions.²²

Acknowledgment. Financial support of this work by the Fonds der Chemischen Industrie and the Deutsche Forschungsgemeinschaft is gratefully acknowledged.

Supporting Information Available: CIF files giving full crystallographic data for **5a,b** and **7a'**. This material is available free of charge via the Internet at <http://pubs.acs.org>.

OM0701726

(21) ASTRO, SAINT and SADABS: Data Collection and Processing Software for the SMART System; Siemens Analytical X-ray Instruments Inc., Madison, WI, 1996.

(22) Sheldrick G. M. SHELXL-97, Program for Crystal Structure Determination; University of Göttingen, Göttingen, Germany, 1997.